Cell, Vol. 89, 1155–1164, June 27, 1997, Copyright ©1997 by Cell Press

Coassembly of TRP and TRPL Produces a Distinct Store-Operated Conductance

Xian-Zhong Shawn Xu,*‡ Hong-Sheng Li,*‡ William B. Guggino,† and Craig Montell*

*Department of Biological Chemistry
Department of Neuroscience
†Department of Physiology
The Johns Hopkins University School of Medicine
Baltimore, Maryland 21205

Summary

The Drosophila retinal-specific protein, TRP (transient receptor potential), is the founding member of a family of store-operated channels (SOCs) conserved from C. elegans to humans. In vitro studies indicate that TRP is a SOC, but that the related retinal protein, TRPL, is constitutively active. In the current work, we report that coexpression of TRP and TRPL leads to a store-operated, outwardly rectifying current distinct from that owing to either TRP or TRPL alone. TRP and TRPL interact directly, indicating that the TRP–TRPL-dependent current is mediated by heteromultimeric association between the two subunits. We propose that the light-activated current in photoreceptor cells is produced by a combination of TRP homo- and TRP–TRPL heteromultimers.

Introduction

Store-operated Ca^{2+} entry (SOCE), the process by which transient release of Ca^{2+} from the internal stores leads to a sustained plasma membrane Ca^{2+} conductance (Putney, 1986), is widespread and has been detected in nearly every mammalian cell type that has been specifically examined for this mode of Ca^{2+} entry (reviewed in Putney and Bird, 1993; Berridge, 1995). SOCE functions both in excitable cells, as well as in nonexcitable cells, where it may be the primary mode of Ca^{2+} entry. Ca^{2+} entry into cells via SOCE is not constitutive but is a highly regulated process activated by a variety of agonists, such as hormones, growth factors, and light, which stimulate production of inositol 1,4,5-trisphosphate (IP_3) and release of Ca^{2+} from the internal pools. As such, SOCE is likely to play a key role in signaling during development, as well as in the fully differentiated animal. Specifically, SOCE has been implicated in T cell activation, osteoclast function, mitogenesis in fibroblasts, and Drosophila phototransduction (reviewed in Berridge, 1995).

Among the best-characterized store-operated conductances is I_{CRAC}, a current with a low conductance but high Ca^{2+} selectivity (Lewis and Cahalan, 1989; Hoth and Penner, 1992; McDonald et al., 1993). However, recent studies indicate that a variety of store-operated currents exist that display a diversity of cation selectivity and conductance characteristics. These include currents that are also Ca^{2+} selective but display higher conductances than I_{CRAC} (Lückhoff and Clapham, 1994), as well as store-operated nonselective cation currents (Krause et al., 1996). This diversity may be generated from a large number of distinct channel proteins. Alternatively, it is possible that coassembly of store-operated channels (SOCs) may be critical in formation of many of the observed conductances.

The Drosophila *trp* locus, which is expressed specifically in the visual system (Montell et al., 1985), appears to encode the archetypical SOC (Vaca et al., 1994; Peterson et al., 1995). Mutations in *trp* result in a severe defect in Drosophila vision (Cosens and Manning, 1969), a process that utilizes the inositol phospholipid signaling system (reviewed in Minke and Selinger, 1996). In contrast to wild type, *trp* photoreceptor cells fail to sustain a response to bright light (Cosens and Manning, 1969). In wild type, there appears to be at least two currents, one of which is more Ca^{2+} selective than the other. The *trp* phenotype appears to be due to a dramatic decrease in Ca^{2+} influx owing to a defect in the more Ca^{2+}-selective conductance (Hardie and Minke, 1992).

The *trp* gene product is a protein of 1275 amino acids with multiple transmembrane domains (Montell and Rubin, 1989; Wong et al., 1989), a feature reminiscent of many members of the superfamily of voltage- and second messenger–gated ion channels (reviewed in Jan and Jan, 1992). Another retinal-specific protein, TRPL, has been identified, which is ~40% identical to TRP over the N-terminal ~700 amino acids (Phillips et al., 1992). Recently, proteins homologous to TRP have been described in organisms ranging from C. elegans to humans (Peterson et al., 1995; Wes et al., 1995; Zhu et al., 1995). Although the cellular distributions of the vertebrate TRPC proteins have not yet been described, many tissues, including the brain, express multiple *TRPC* genes (Peterson et al., 1995; Wes et al., 1995; Zhu et al., 1995, 1996; Philipp et al., 1996).

Several TRPC proteins have now been functionally expressed and shown to display characteristics of a SOC. Drosophila TRP and TRPL have been most extensively studied, primarily in Sf9 cells and Xenopus oocytes, and it appears that the channel formed by TRP is a SOC (Hu et al., 1994; Vaca et al., 1994; Peterson et al., 1995). A TRP-dependent conductance, with modest selectivity for Ca^{2+}, can be activated by Ca^{2+} release from the internal stores. However, in vitro studies indicate that TRPL is not a SOC but is a constitutively active cation channel with relatively little ion specificity (Hu et al., 1994). Recently, three vertebrate TRPC proteins, TRPC1, TRPC3 (also referred to as hTRP1 and hTRP3, respectively), and bCCE have been functionally expressed in mammalian tissue-culture cells, and each appears to be activated by release of Ca^{2+} from the internal stores (Philipp et al., 1996; Zhu et al., 1996; Zitt et al., 1996). Thus, the TRPC family appears to include multiple SOCs.

The functional analyses, combined with the observations that there are multiple TRPC proteins, some of

‡These authors contributed equally to this work.

which are expressed in the same tissues, raise the possibility that the TRPC proteins may form heteromultimeric complexes. This proposal is particularly pertinent with respect to TRP and TRPL, since they are both photoreceptor cell specific (Montell et al., 1985; Phillips et al., 1992) and spatially localized to the same subcellular compartment, the microvillar portion of the photoreceptor cells, referred to as rhabdomeres (Niemeyer et al., 1996; Chevesich et al., 1997). Such heteromultimerization could potentially be important in defining novel channel characteristics, as has been shown to be the case among the K^+ channel family (reviewed in Salkoff et al., 1992). Recently, there has been a suggestion that there may be a synergistic interaction between TRP and TRPL (Gillo et al., 1996), raising the question as to whether these two channels coassemble to form a functional SOC.

In the current report, we show that TRP and TRPL coassembled in 293T cells to produce a SOC with a combination of properties exhibited by the homomeric channels. The TRP–TRPL current exhibited many of the features characteristic of the light-induced conductance in Drosophila photoreceptor cells. The TRP and TRPL proteins associated directly in 293T cells, suggesting that the two proteins formed a novel channel. Additional evidence that TRP and TRPL interacted as homo- and heteromultimers was that the functional activity of the TRP channel was suppressed by a dominant-negative form of TRPL and vice versa. We further showed that the N-terminal and transmembrane domains contributed to subunit assembly.

Results

Coimmunoprecipitation of TRP and TRPL In Vivo and In Vitro

To address whether TRP and TRPL interact in vivo, we tested whether the two proteins coimmunoprecipitated (co-IPed) from Drosophila photoreceptor cells. Extracts were prepared from fly heads and IPed with anti-TRP antibodies or nonimmune serum. The immune complexes were then fractionated by SDS–PAGE, and a Western blot was probed with anti-TRPL antibodies. TRPL was detected in extracts IPed with anti-TRP antibodies but not in the control IP using nonimmune serum (Figure 1A).

To develop an in vitro-assay system for mapping the domains involved in subunit interaction and for testing the possible functional consequences of coassembly of TRP and TRPL, we tested whether TRP and TRPL co-IPed after coexpression of the two proteins in 293T cells (DuBridge et al., 1987). Extracts were IPed with anti-TRP antibodies, and Western blots of the immune complexes were probed with anti-TRPL antibodies. TRPL was detected in extracts prepared from cells expressing both proteins but not in a control using nonimmune serum or from control cells expressing just TRPL (Figure 1B). TRPL was expressed to a similar extent in cells expressing both TRP and TRPL or TRPL alone (Figure 1B, lysate lanes). Therefore, the ability to detect TRPL after IPing with anti-TRP antibodies was not a secondary consequence of increased stability of TRPL in cells expressing

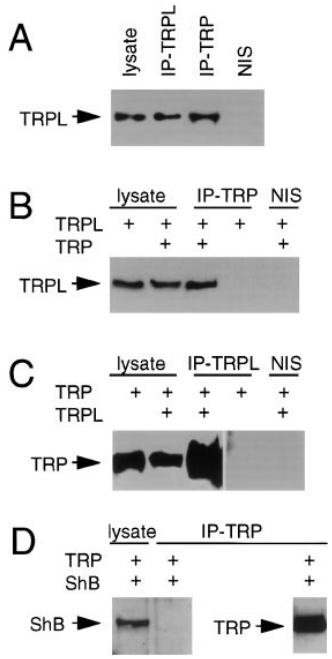

Figure 1. Coimmunoprecipitation of TRP and TRPL In Vivo and In Vitro

(A) Co-IP of TRP and TRPL from Drosophila photoreceptor cells. Total head extracts (lysate; 3 heads) or immune complexes obtained using anti-TRPL antibodies (IP-TRPL; 12 heads), anti-TRP antibodies (IP-TRP; 60 heads), or nonimmune serum (NIS; 60 heads) were fractionated by SDS–PAGE, and the Western blot was probed with anti-TRPL antibodies.

(B and C) pTRP and pTRPL constructs were singly or cotransfected into 293T cells (indicated by [+] above each lane). Cell lysates were IPed with (B) anti-TRP or (C) anti-TRPL antibodies or nonimmune serum (indicated by IP-TRP, IP-TRPL, or NIS, respectively). Western blots of the immune complexes were probed with (B) anti-TRPL or (C) anti-TRP antibodies. Expression of (B) TRPL and (C) TRP in transfected 293T cells was checked by probing Western blots of total cell lysates (lysate).

(D) pTRP and pShaker B were cotransfected into 293T cells and IPed with anti-TRP antibodies, and a Western blot of the immune complexes (IP-TRP), as well as the total cell lysate (lysate), was probed with anti-Shaker B antibodies. The exposure time of the right lane in panel (D) was 10× shorter than that of the two left lanes. (B) and (C) were from independent experiments.

both proteins. In a reciprocal experiment, cells were cotransfected with either both proteins or just TRP, and the extracts were IPed with anti-TRPL antibodies. In this latter experiment, TRP also co-IPed with TRPL (Figure 1C). The association of TRPL with TRP did not appear to be due to nonspecific interactions between two membrane proteins since Shaker B and TRP did not co-IP when expressed in 293T cells (Figure 1D).

Coexpression of TRP and TRPL Produced a Store-Operated Outwardly Rectifying Conductance

To determine the functional consequences of the direct association between TRP and TRPL, we performed whole-cell recordings from 293T cells that were singly or cotransfected with TRP and/or TRPL. 293T cells were selected for these studies since, in contrast to Xenopus

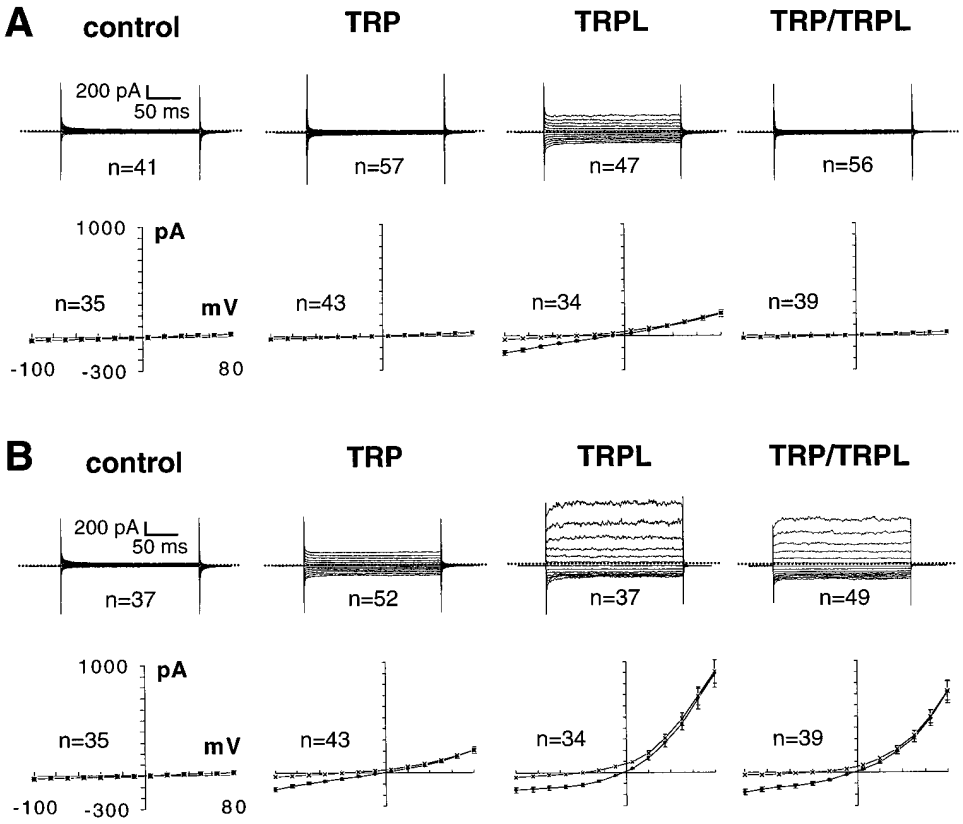

Figure 2. TRP, TRPL, and TRP–TRPL Currents in 293T Cells before and after Thapsigargin Treatment

Twice the concentration of *TRP* versus *TRPL* cDNA constructs, pTRP and pTRPL, were used in either single or cotransfection experiments. (A) Currents before TG treatment. Upper traces show currents produced by bathing the cells in an Na^+ solution and applying a set of step voltages from −100 to +80 mV in 15 mV increments. The holding potential was −10 mV. Dotted lines indicate 0 pA. Lower plots are the I–V relationships of the currents obtained from cells bathed in either Na^+ (dots) or NMDG (crosses) solution. Shown are the mean data, as well as the SDs (indicated by the brackets through the mean values in the I–V graphs). The numbers of cells analyzed (n) are indicated.

(B) Currents recorded after depleting the intracellular Ca^{2+} stores by perfusing the cells for 7–10 min with a Ca^{2+}-free solution containing 1 μM TG. The data were obtained as described in part (A). The I–V analyses in parts (A) and (B) were obtained from the same cells.

oocytes and Sf9 cells, they displayed very low levels of cation influx either in the absence or presence of thapsigargin (Figures 2A and 2B), an agent that inhibits the Ca^{2+}-ATPase in the IP_3-sensitive Ca^{2+} stores and results in net Ca^{2+} release from the internal stores via the leak current (Jackson et al., 1988). Cells were cotransfected with a marker gene, *CD4*, to identify those cells that were efficiently transfected and likely to express TRP and/or TRPL. Cells that expressed the marker protein and were similar in diameter and shape, and therefore capacitance (19.3–22.1 pF), were analyzed at holding potentials ranging from −100 to +80 mV.

In accordance with previous studies in Sf9 cells (Vaca et al., 1994), introduction of TRP into 293T cells resulted in a thapsigargin-induced cation influx. No detectable TRP-dependent current was observed in the absence of thapsigargin (Figure 2A). The thapsigargin-dependent current (Figure 2B) was inhibited ~50% by 1.2 mM Mg^{2+} or 80 μM La^{3+} (Table 1; Figure 3). Although the relative permeability to Ca^{2+} was 10-fold greater than to Na^+ (Table 1), Na^+ was used as the permeant ion since the currents were larger with Na^+ alone, apparently owing to Ca^{2+}-mediated inactivation of the channel (Figure 3). The small inward current in NMDG solution was due to the leak current. The observation that TRP activity was thapsigargin dependent in 293T cells was consistent with previous studies indicating that TRP was a SOC.

In contrast to TRP, TRPL expressed in 293T cells exhibited constitutive activity similar to that previously described (Hu et al., 1994). However, we found that in the presence of thapsigargin there appeared a large outwardly rectifying current (Table 1; Figure 2B). Outward rectification is also a feature of the light-activated current in flies, though the relative permeabilities, P_{Ca}:P_{Na}, of the TRPL current in 293T cells were lower than in photoreceptor cells (3.5:1 as opposed to ~25–40:1; Table 1) (Hardie, 1991; Hardie and Minke, 1992), and the activity in the absence of thapsigargin was not typical of a SOC. TRPL was inactivated by Ca^{2+} to a similar extent as TRP; however, the inhibition by Mg^{2+} or La^{3+} was minimal (Table 1; Figure 3).

Of primary significance here, we found that coexpression of TRP and TRPL resulted in the production of a novel current exhibiting certain features typical of TRP and others most similar to TRPL. As was the case with TRP alone, current was only detected in the presence of thapsigargin in ~95% of those cells analyzed (Figure 2B). Thus, the current did not appear to be due to TRPL

Table 1. Characteristics of TRP, TRPL, and TRP-TRPL Channels

	P_{Ca}:P_{Na}	Percentage of Mg^{2+} Inhibition (%)	Percentage of La^{3+} Inhibition (%)	Current (pA) at −100 mV	Current (pA) at +80 mV
TRP	10.2 ± 0.8 (n = 15)	49.7 ± 11.3 (n = 43)	53.7 ± 14.3 (n = 27)	137.3 ± 29.3 (n = 43)	169.1 ± 29.7 (n = 43)
TRPL (no TG)	2.7 ± 0.8 (n = 4)	13.3 ± 8.2 (n = 29)	0.6 ± 0.7 (n = 36)	139.6 ± 25.9 (n = 34)	187.3 ± 33.9 (n = 34)
TRPL	3.5 ± 0.9 (n = 9)	14.9 ± 9.8 (n = 21)	0.7 ± 0.9 (n = 31)	142.8 ± 30.6 (n = 34)	871.5 ± 141.3 (n = 34)
TRP–TRPL	11.5 ± 1.1 (n = 10)	57.6 ± 10.7 (n = 33)	6.8 ± 4.3 (n = 29)	167.9 ± 31.7 (n = 39)	714.2 ± 117.4 (n = 39)

The percentage of Mg^{2+} or La^{3+} inhibition was calculated from currents at −60 mV in the absence or presence of 1.2 mM $MgCl_2$ or 80 μM $LaCl_3$, respectively. The P_{Ca}:P_{Na} values and SDs were obtained as described in Experimental Procedures. The numbers of cells analyzed is indicated (n).

alone, since TRPL is constitutively active. Several other properties were also similar to TRP, including the relative permeability, P_{Ca}:P_{Na}, inactivation by Ca^{2+}, and inhibition by Mg^{2+} (Table 1; Figure 3). However, the TRP–TRPL current displayed a large outward rectification that was only slightly smaller than that characteristic of TRPL alone (Table 1; Figure 2B). Thus, the TRP–TRPL current did not appear to be due to TRP alone. Furthermore, the TRP–TRPL current was as insensitive to 80 μM La^{3+} as TRPL (Table 1). As coexpression of TRP with TRPL suppressed the constitutive activity of TRPL, this suggested that the two proteins interacted directly to form heteromultimers. We occasionally observed cells that displayed currents that were constitutively active and that were indistinguishable from those generated by TRPL alone (~5%). We also occassionally detected currents (~5%) with a linear I–V relationship that were reminiscent of TRP alone (data not shown). These latter currents may have reflected some cells that expressed just one rather than both proteins.

Domains Involved in Subunit Association

Several assays were used to discern which domains of TRP and TRPL functioned in subunit interaction. In the first assay, we used the yeast two-hybrid system (Fields and Song, 1989). The N- and C-terminal domains of TRP (Figure 4A) were subcloned into vectors containing either the yeast GAL4 DNA-binding domain or the activation domain and introduced into a *his*$^-$ strain of yeast.

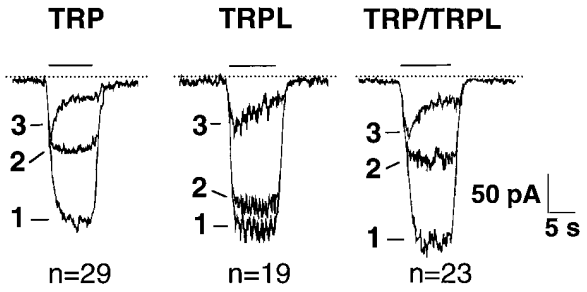

Figure 3. Ca^{2+} Inactivation and Mg^{2+} Inhibition of TRP, TRPL, and TRP–TRPL Currents

The inward currents were recorded at −60 mV after treating the cells with 1 μM TG as described in Figure 2. The dotted lines indicate 0 pA. The cells were initially bathed in an NMDG solution and then in the following solutions as indicated: 1, Na^+; 2, Na^+ and Mg^{2+}; and 3, Na^+, Mg^{2+}, and Ca^{2+}. The concentrations of Na^+, Mg^{2+}, and Ca^{2+} were 140 mM, 1.2 mM and 2.5 mM, respectively. Each set of superimposed traces were obtained from the same cell. The numbers of cells characterized is indicated (n).

Interaction between the N- and C-terminal domains of TRP were then identified on the basis of growth on *his*$^-$ media. Growth was only observed when both the GAL4 DNA-binding and -activation domains were fused to the N-terminus of TRP (Table 2). Similar results were obtained with the corresponding N- and C-terminal domains of TRPL (Figure 4B; Table 2). We also considered whether TRP and TRPL were involved in heterotypic interaction. We found that growth on *his*$^-$ media was also observed when the N-terminal domains of TRP and TRPL (N-TRP and N-TRPL, respectively) were fused to the DNA-binding domain and activation domains and vice versa (Table 2). These results indicated that there were homophilic and heterophilic interactions between TRP and TRPL, and these interactions were mediated, at least in part, through the N-terminal regions.

Column-binding assays were also used to address whether N-TRP and N-TRPL were important in subunit interaction. N-TRP and N-TRPL were expressed in E. coli as GST fusion proteins (GST-N-TRP and GST-N-TRPL, respectively), and equal quantities of both proteins were bound to glutathione columns. N-TRP and N-TRPL were labeled in vitro with ^{35}S, and equal amounts of each probe were passed over each column. The ^{35}S-labeled N-TRP and N-TRPL were eluted with glutathione and detected after fractionating the proteins by SDS–PAGE. Both [^{35}S]N-TRP and [^{35}S]N-TRPL bound to GST-N-TRP and GST-N-TRPL but not to columns containing a 2-fold excess of GST alone (Figures 4C and 4D). Approximately 5-fold more [^{35}S]N-TRP consistently bound to the GST-N-TRPL than the GST-N-TRP (Figure 4C). The converse results were obtained using [^{35}S]N-TRPL; 5-fold more probe bound to GST-N-TRP than GST-N-TRPL (Figure 4D).

Additional evidence that N-TRP and N-TRPL played roles in subunit assembly was obtained in co-IP experiments. N-TRP and N-TRPL, linked to MYC tags, were co-transfected with full-length TRP, and the extracts were IPed with anti-TRP antibodies and probed with anti-MYC antibodies. The results of the analysis demonstrated that N-TRP and N-TRPL co-IPed with full-length TRP (Figures 4E and 4F). To determine whether N-TRP could also co-IP with just the N-terminal regions of either TRP or TRPL, two forms of N-TRP, fused to MYC or FLAG tags, were coexpressed in 293T cells. We found that N-TRP-FLAG co-IPed with either N-TRP-MYC (Figures 4G) or N-TRPL-MYC (Figure 4H). Thus, on the basis of the yeast two-hybrid assay, column-binding studies, and coimmunoprecipitation experiments, it appeared that TRP and TRPL formed heteromultimers, and this interaction was mediated in part by the N-terminal domains.

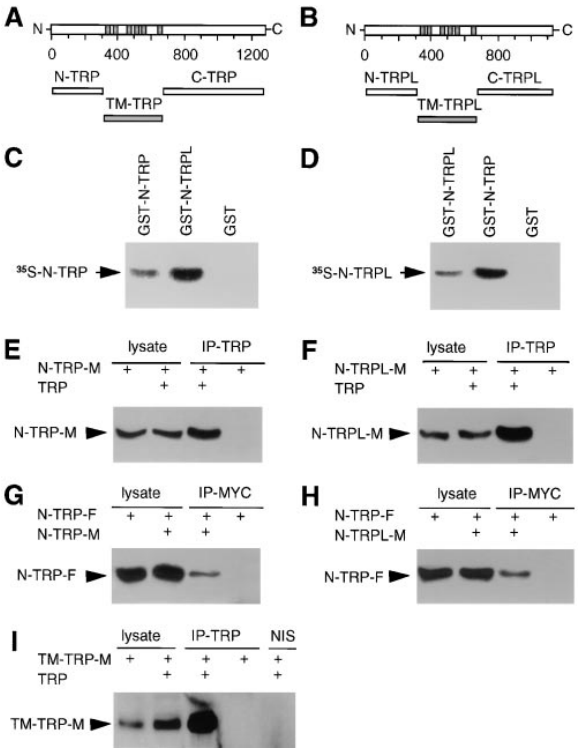

Figure 4. Homo- and Heteromultimeric Binding of N-Terminal and Transmembrane Domains of TRP and TRPL

(A) Schematic of TRP domains. The top bar represents TRP. A scale, in amino acids, is indicated. The six dark vertical boxes represent the putative transmembrane (TM) domains. The portions of TRP included in the N-TRP (residues 1–333), TM-TRP (residues 324–672), and C-TRP (residues 661–1275) proteins are indicated.

(B) Schematic of TRPL domains: N-TRPL (residues 1–338) and C-TRPL (residues 676–1114).

(C and D) Column-binding assays. Equal amounts of purified N-TRP and N-TRPL fused to GST (GST-N-TRP or GST-N-TRPL, respectively) or 2-fold more of GST were immobilized on glutathione beads and incubated with equal amounts of (C) N-TRP or (D) N-TRPL labeled with [^{35}S]methionine. The beads were washed and the proteins were eluted with glutathione. The eluted proteins were fractionated by SDS–PAGE, and the ^{35}S-labeled proteins were detected using a phosphoimager.

(E–I), Co-IP assays indicated that the N-terminal and TM regions of TRP were involved in subunit assembly. (E) Plasmids encoding MYC-tagged N-terminal TRP (N-TRP-M) or (F) MYC-tagged N-terminal TRPL (N-TRPL-M) were transfected alone or with pTRP (indicated by [+] above each lane). Cell lysates were IPed with anti-TRP antibodies, and Western blots of the immune complexes (IP-TRP) and total cell lysates (lysate) were probed with anti-MYC antibodies. (G) and (H) FLAG-tagged N-terminal TRP (N-TRP-F) was singly or cotransfected with MYC-tagged N-terminal TRP (N-TRP-M) or MYC-tagged N-terminal TRPL (N-TRPL-M). Cell lysates were IPed with anti-MYC antibodies, and Western blots of the immune complexes (IP-MYC) and total cell lysates (lysate) were probed with anti-FLAG antibodies. (I) Plasmid encoding the MYC-tagged TM domains of TRP (TM-TRP-M; residues 324–672) was transfected alone or with pTRP, and the cell lysates were IPed with anti-TRP antibodies (IP-TRP) or nonimmune serum (NIS). Western blot of the immune complexes and total cell lysates were probed with anti-MYC antibodies.

To determine whether the transmembrane domains also functioned in TRP subunit assembly, we coexpressed full-length TRP along with the TRP transmembrane domains fused to a MYC tag (TM-TRP-MYC). TRP was subsequently IPed from the cell extracts, and protein blots were probed with anti-MYC antibodies. A strong signal corresponding to TM-TRP-MYC was detected in the IPs, but not from control cells expressing just TM-TRP-MYC or from extracts containing both proteins after IPing with nonimmune serum (Figure 4I). These results suggested that the transmembrane domains also promoted subunit assembly.

Table 2. N-Terminal Domains of TRP and TRPL Interacted in a Yeast Two-Hybrid Assay

GAL4-BD	GAL4-AD	Growth on *his*$^-$ Plate
N-TRP	N-TRP	+
N-TRP	C-TRP	−
C-TRP	C-TRP	−
N-TRPL	N-TRPL	+
N-TRPL	C-TRPL	−
C-TRPL	C-TRPL	−
N-TRP	N-TRPL	+
N-TRPL	N-TRP	+

Plasmids containing the N- or C-terminal regions of TRP or TRPL were fused to the GAL4 DNA-binding domain (GAL4-BD) or to the GAL4-activation domain (GAL4-AD) and transformed into the yeast strain HF7c in combination as shown. Growth on SD-*trp*$^-$, *leu*$^-$, *his*$^-$ media is indicated (+).

Dominant Suppression of TRP and TRPL

To investigate further the functional significance of the N-terminal interactions, we tested whether overexpression of N-TRP and N-TRPL could dominantly suppress the TRP current. We found that the coexpression of either N-TRP or N-TRPL dominantly suppressed TRP ~75% (Figure 5). The incomplete inhibition of the TRP current may have been due to the absence of the transmembrane segments in the dominant-negative constructs. Therefore, we designed potentially dominant-negative forms of TRP and TRPL, which included the N-terminal and transmembrane domains, by replacing the putative pore domains in TRP and TRPL with H5 from Shaker B (Hartmann et al., 1991; Yellen et al., 1991; Yool and Schwarz, 1991). Mutations in H5 of an inwardly rectifying K^+ channel, IRK1, dominantly suppresses the current from wild-type IRK1 (Tinker et al., 1996), raising the possibility that perturbation of the putative H5 in TRP and TRPL would have similar effects. Substitution of the H5 region of either TRP or TRPL with the Shaker

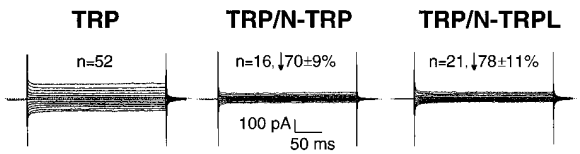

Figure 5. Inhibition of the TRP-Dependent Current by N-TRP and N-TRPL

293T cells were either singly transfected with pTRP or cotransfected with pN-TRP or pN-TRPL in combination with pTRP. The ratios of pN-TRP:pTRP and pN-TRPL:pTRP were 3:1. The currents were recorded after depleting the Ca^{2+} stores with 1 μM TG as described in Figure 2. The dotted lines indicate 0 pA. The number of cells analyzed (n) and the percent inhibition of the TRP-dependent current (determined at −100 mV) is indicated to the right of the inverted arrow.

B H5 domain (creating TRP-K and TRPL-K, respectively) caused complete loss-of-function of TRP and TRPL activity, since the cells transfected with these constructs were indistinguishable from nontransfected control cells (Figure 6). Most importantly, TRP-K or TRPL-K dominantly inhibited the activity of either wild-type TRP or TRPL ~95% (Figure 6), indicating that TRP and TRPL formed both homo- and heteromultimers.

Coimmunoprecipitation of TRPC1 and TRPC3

The observation that TRP and TRPL form heteromultimeric interactions raises the possibility that members of the vertebrate TRPC family also assemble into heteromultimeric complexes. Human TRPC1 and TRPC3 are both expressed in the adult brain (Wes et al., 1995; Zhu et al., 1995, 1996), although it is not known whether they are expressed in the same cells. To determine whether TRPC1 and TRPC3 interact, we completed the partial TRPC3 sequence that we previously reported (Wes et al., 1995) and found that TRPC3 was expressed as a protein of 848 amino acids (data not shown). The only deviation from the complete TRPC3 sequence recently reported (Zhu et al., 1996) was an alanine-to-glutamic acid substitution in residue 820. Full-length TRPC1 and TRPC3, fused to FLAG and MYC tags, respectively, were coexpressed in 293T cells. TRPC1 or TRPC3 was then IPed with either anti-FLAG or anti-MYC antibodies, and Western blots containing the immune complexes were probed with the reciprocal antibodies. The results of this analysis demonstrated that TRPC1 and TRPC3 co-IPed, suggesting that TRPC1 and TRPC3 may form heteromultimeric complexes (Figure 7).

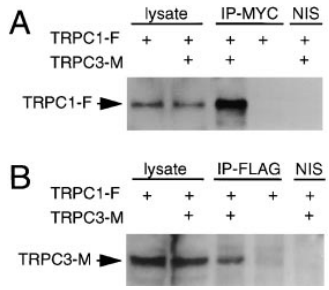

Figure 7. Coimmunoprecipitation of TRPC1 and TRPC3

Plasmids encoding FLAG-tagged TRPC1 (TRPC1-F) and MYC-tagged TRPC3 (TRPC3-M) were transfected into 293T cells either together or individually. Cell lysates were processed for Western analysis directly or used for IPs.

(A) Cell lysates were IPed with anti-MYC monoclonal antibodies (IP-MYC) or nonimmune serum (NIS), and Western blots of total cell lysates (lysate) and the immune complexes were probed with anti-FLAG antibodies.

(B) Cell lysates were IPed with anti-FLAG antibodies (IP-FLAG) or NIS, and Western blots of total cell lysates and the immune complexes were probed with anti-MYC antibodies.

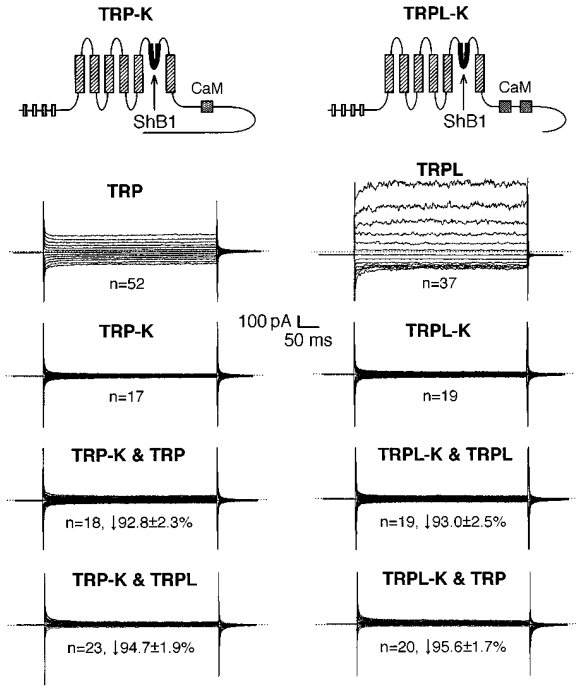

Figure 6. Dominant Suppression of the TRP- and TRPL-Dependent Currents with TRP-K and TRPL-K

Cells were either singly transfected with pTRP or pTRPL or cotransfected with pTRP or pTRPL and plasmids encoding the nonfunctional chimeras TRP-K and TRPL-K. The schematic represents the chimeric proteins TRP-K and TRPL-K containing the putative pore domains of Shaker B (indicated by the closed loops). Equal amounts of each plasmid were used in the single transfections. In the cotransfections, a 3-fold excess of pTRP-K and pTRPL-K was used relative to pTRP and pTRPL. The currents were recorded after TG treatment as described in Figure 2. The dotted lines indicate 0 pA. The number of cells analyzed (n) and the percent inhibition of the TRP-dependent current (determined at −100 mV) is indicated to the right of the inverted arrow.

Discussion

TRP Homo- and TRP–TRPL Heteromultimers Form Functional SOCs

TRP has emerged as the archetypical member of a rapidly growing family of related proteins, conserved from C. elegans to humans, which appear to be SOCs. However, TRPL, which shares considerable sequence identity with TRP, has been reported to be constitutively active in vitro and insensitive to release of Ca^{2+} from the internal stores (Hu et al., 1994). Thus, the question arises as to whether only a subset of the TRP-related proteins are SOCs. Alternatively, TRPL may be one subunit of a SOC and require an additional protein to impart the store-operated regulation. A recent study in Xenopus oocytes provided a suggestion that there may be a cooperative interaction between TRP and TRPL, since coexpression of TRP and TRPL produced an inward Mg^{2+} current (Gillo et al., 1996). However, this study did not address whether the apparent synergistic effect was due to direct interaction of TRP and TRPL or to coexpression of separate TRP and TRPL channels in the same cells. Moreover, in contrast to the currents observed in Drosophila photoreceptor cells, the inward current in oocytes did not carry Na^{+}; instead, Mg^{2+} appeared to be the sole permeant ion and only at hyperpolarizations more extreme than appear to occur in vivo.

In the present work, we found that TRP and TRPL

coimmunoprecipitated from photoreceptor cells. Furthermore, TRP and TRPL coassembled in vitro to produce a current that was distinct from those produced by either protein alone but displayed many characteristics of the in vivo current as discussed below. TRP and TRPL, in addition to assembling into heteromultimeric complexes also were capable of forming homomultimers in 293T cells. Evidence that the individual TRP- and TRPL-dependent currents were due to formation of homomultimers, rather than a monomer, was that the currents were suppressible by dominant-negative forms of TRP or TRPL.

Consistent with the proposal that TRP forms a functional channel in the absence of TRPL, in vivo, is the *trpl* mutant phenotype. Disruption of the TRPL protein in *trpl* flies has no discernible impact on phototransduction (Niemeyer et al., 1996). However, TRPL does function in Drosophila photoreceptor cells, since the phenotype of *trpl; trp* double mutants is much more severe than that of *trp* flies. In such double-mutant flies, the light response is substantially, although not completely, eliminated.

We propose that in Drosophila photoreceptor cells, TRPL only exists as a heteromultimer. Several observations support this proposal: (i) TRPL expressed in vitro does not form a SOC but is constitutively active, whereas TRP–TRPL heteromultimers are regulated by release of Ca^{2+} from the internal stores; (ii) TRP and TRPL coimmunoprecipitated from Drosophila photoreceptor cells; (iii) TRP–TRPL associations appeared to be favored over the TRPL–TRPL interactions in the column-binding assay; finally, (iv) in Drosophila photoreceptor cells, it appears that TRP is considerably ($>$10-fold) more abundant than TRPL (X.-Z. S. X., H.-S. L., and C. M., unpublished data). On the basis of these considerations, it seems likely that most, if not all, of the TRPL monomers complex with TRP. Thus, two classes of ion channels likely to function in Drosophila vision are TRP homomultimers and TRP–TRPL heteromultimers, both of which appear to be regulated by release of Ca^{2+} from the internal stores.

TRP and TRP–TRPL Share Many Features of Light-Activated Current

The light-activated current appears to require release of Ca^{2+} from internal stores (Arnon et al., 1997), is strongly outwardly rectifying, and is more permeable to Ca^{2+} than Na^{+} (Hardie and Minke, 1992). The combination of TRP homomultimers and TRP–TRPL heteromultimers better accounts for these characteristics of the light-induced conductance than expression of TRP and TRPL homomultimers. TRP, expressed in vitro, is activated by a store-operated mechanism and is primarily permeable to Ca^{2+}; however, unlike the light-induced current, the in vitro TRP-dependent current is not outwardly rectifying. TRPL is outwardly rectifying in vitro but displays significant constitutive activity rather than activation by release of Ca^{2+} from the internal stores. In contrast, the TRP–TRPL current is store-operated, more permeable to Ca^{2+} than Na^{+}, and outwardly rectifying. Therefore the TRP–TRPL heteromultimer could account, in part, for the seemingly conflicting observations that in photoreceptor cells the light-induced current, which is primarily permeable to Ca^{2+}, is primarily outwardly rectifying but that the TRP homomultimer expressed in vitro displays a linear current–voltage relationship.

Another feature of the light-sensitive current is inhibition by Ca^{2+} (Hardie and Minke, 1994). Ca^{2+} inhibition of the light-sensitive current could be due to inactivation of TRP and TRP–TRPL and/or feedback inhibition of other proteins associated with TRP. TRP forms a large signaling complex that includes the PDZ domain containing protein INAD (Huber et al., 1996a; Shieh and Zhu, 1996), the phospholipase C β encoded by *norpA* (Huber et al., 1996b; Chevesich et al., 1997), rhodopsin, and calmodulin (Chevesich et al., 1997). We have proposed that the function of linking TRP directly to calmodulin, and indirectly to RH1 and NORPA via INAD, may be to facilitate feedback regulation of these proteins by holding them in proximity to the TRP-dependent Ca^{2+} flux (Chevesich et al., 1997). Consistent with this proposal, and the findings that the light-sensitive channels in Drosophila photoreceptor cells are inactivated by Ca^{2+}, we found that Ca^{2+} appeared to inactivate the conductances of TRP alone, as well as of TRP–TRPL. Furthermore, Ca^{2+}-dependent inactivation may be common to the vertebrate SOCs, since I_{CRAC}, a highly Ca^{2+}-selective store-operated conductance, is inactivated by Ca^{2+} (McDonald et al., 1993; Zweifach and Lewis, 1995).

In addition to Ca^{2+}, physiological concentrations of Mg^{2+} also inhibit the light-sensitive conductance in Drosophila photoreceptors (Hardie and Mojet, 1995). These observations have parallels to the vertebrate light-sensitive channels, which are also inhibited by Ca^{2+} and Mg^{2+} (Nakatani and Yau, 1988). It has been proposed that the Mg^{2+} block is an important factor in improving the signal-to-noise ratio in both vertebrate and Drosophila photoreceptors (Hardie and Mojet, 1995). In Drosophila, the Mg^{2+} block was largely, although not completely, relieved in whole-cell recordings of *trp* photoreceptors. This suggests that the inhibition by Mg^{2+} is mediated by TRP. Consistent with these in vivo studies, we found that the TRP and TRP–TRPL conductances were reduced $\sim$50% by physiological levels of Mg^{2+}; however, the TRPL conductance was relatively insensitive to Mg^{2+}.

The TRP current in photoreceptor cells also appears to be inhibited by La^{3+}, since the TRP phenotype can be largely mimicked by application of La^{3+} (Suss-Toby et al., 1991). The remaining current in TRP mutant flies is La^{3+} insensitive. Thus, there appears to be at least two types of currents in photoreceptor cells, only one of which is inhibited by La^{3+}. In 293T cells, the TRP but not the TRP–TRPL current is La^{3+} sensitive. Thus, the effects of Ca^{2+}, Mg^{2+}, and La^{3+} on TRP and TRP–TRPL, and the outward rectification of TRP–TRPL in 293T cells, are properties they share with the light-sensitive current in photoreceptor cells.

A conundrum that remains to be resolved is an explanation for the findings that the photoresponse of *trpl* flies is indistinguishable from wild type; yet, *trpl; trp* double mutants exhibit a more severe phenotype than *trp* (Niemeyer et al., 1996). In the double mutants, there remains a very small but detectable light-induced current. To reconcile these observations, we propose that a third TRP-related (TRPR) protein is expressed in photoreceptor cells, which displays very little activity on its

own but that forms heteromultimers with TRPL and TRP. The remaining response in *trp* mutant flies may be due to heteromultimeric association between TRPL and TRPR. No phenotype may be detected in *trpl* mutants owing to functional redundancy of the TRP–TRPL and TRP–TRPR heteromultimers. Moreover, both TRP–TRPL and TRPR–TRPL may contribute to the remaining current in photoreceptor cells after application of La^{3+}.

Vertebrate TRPC Channels May Form Heteromultimers

Mice and humans express multiple TRPC proteins (Wes et al., 1995; Zhu et al., 1995, 1996), raising the possibility that there may be heteromultimeric interaction among the vertebrate TRP homologs that contributes to functional diversity. The heteromultimeric interaction between TRPC1 and TRPC3 described in the current report may result in current characteristics distinct from the individual components, as well as conferring upon TRPC1 regulation by release of Ca^{2+} from the internal stores. Although TRPC1 and TRPC3 are store operated when expressed in mammalian cells (Zhu et al., 1996; Zitt et al., 1996), TRPC1 is constitutively active in the insect cell line, Sf9 cells (Sinkins and Schilling, 1997). This constitutive activity may reflect a requirement for another TRPC protein that is not expressed in Sf9 cells. Thus, there may be vertebrate homologs of TRPL that are constitutively active and require heterotypic interactions with other TRPC proteins for store-operated activity. It will be of interest to characterize further which vertebrate TRPC proteins assemble into heteromultimeric complexes and the functional consequences of such interactions.

Experimental Procedures

DNA Constructs for Expression in 293T Cells

All the constructs used for expression in 293T cells were in the pcDNA3.1 vector (Invitrogen). In each case, the Kozak sequences 5′ to the initiating codon were modified to optimize translation (Kozak, 1984). Some constructs included a MYC or FLAG epitope tag inserted at the N-terminus. pTRP and pTRPL were the full length *trp* and *trpl* cDNAs constructs. pTRP-K and pTRPL-K were made by replacing amino acids 570–633 (from pTRP) or residues 577–640 (from pTRPL) with amino acids 422–455 from pShaker B (Schwartz et al., 1988). pN-TRP (with either a MYC or FLAG tag) and pN-TRPL (with a MYC tag) consisted of TRP and TRPL residues 1–333 and 1–338, respectively. pTM-TRP (with a MYC tag) included TRP residues 324–674. pTRPC1 (with a FLAG tag) began with the initiator methionine reported for hTRP1 and TRPC1A (Zhu et al., 1996; Zitt et al., 1996) and ending at the C-terminus reported for TRPC1, hTRP1, and TRPC1A (Wes et al., 1995; Zhu et al., 1995; Zitt et al., 1996). pTRPC3 (with a MYC tag) consisted of the *TRPC3* cDNA.

Cell Culture and Coimmunoprecipitations

Co-IPs from fly heads were performed as described (Shieh and Zhu, 1996) with minor revisions. In brief, 20 mg of fly heads were homogenized on ice in 0.4 ml SMART buffer (0.2% dodecyl-β-maltoside, 2.7 mM KCl, 10 mM Na_2HPO_4, 1.8 mM KH_2PO_4, 500 mM NaCl, 5 mM EDTA, 5 mM EGTA, 8 mM $MgCl_2$, 2 μg/ml aprotinin, 10 μg/ml leupeptin, 0.1 mM PMSF, 10 mM NaPPi, 50 mM NaF, 1 mM GTP [pH 7.3]) and centrifuged to remove debris. Subsequently, anti-TRP antibodies (Chevesich et al., 1997) or nonimmune serum and 50 μl 1% protein A–agarose were added to the supernatant, which was then rotated at 4°C for 2 hr. The IPs were washed with SMART buffer, eluted with SDS sample buffer, and analyzed by Western analysis.

293T cells (DuBridge et al., 1987) were maintained in DMEM–FCS (37°C, 5.5% CO_2). For consistency in the experiments, the cells were maintained for a limited number of passages (six) after thawing the cells. Transfections were performed using Lipofectamine (BRL). Typically, ~35%–50% of the cells were transfected. Cells from single 100 mm dishes were lysed 36–48 hr posttransfection with 1 ml cold IPB buffer (1% Triton X-100 and protease-inhibitor cocktail [Boehringer Mannheim]) in PBS and centrifuged to remove cellular debris. The subsequent IP protocol was similar to that described (Chevesich et al., 1997) using 0.5 ml supernatant, the appropriate antibodies, and 50 μl protein A–agarose beads or protein G–Sepharose. The mixture was then rotated for 2 hr at 4°C. The IPs were washed with IPB buffer, eluted with SDS sample buffer, fractionated by SDS–PAGE (10% gels except for the 6% gel shown in Figure 1), transferred to PVDF membrane, probed with the appropriate antibodies, and detected by the ECL enhanced chemiluminescence method (Amersham).

Yeast Two-Hybrid Assay

N-TRP (residues 1–333), N-TRPL (residues 1–338), C-TRP (residues 661–1275), and C-TRPL (residues 676–1114) were subcloned into pGBT-9 (GAL4 DNA binding domain; Clonetech) or pGAD424 (GAL4 DNA activation domain; Clonetech). Plasmids were transformed into the yeast reporter strain HF7c (Clonetech). The cells were grown on SD-*trp*$^-$, *leu*$^-$ plates to select transformants and subsequently streaked on both of SD-*trp*$^-$, *leu*$^-$ and SD-*trp*$^-$, *leu*$^-$, *his*$^-$ plates. Growth on SD-*trp*$^-$, *leu*$^-$, *his*$^-$ plates indicated protein–protein interaction.

GST-Affinity Column–Binding Assay

GST-N-TRP and GST-N-TRPL fusion proteins were made by introducing fragments encoding N-TRP (residues 1–333) and N-TRPL (residues 1–338) into pGEX5.1 (Pharmacia). The cultures (100 ml), in E. coli strain BL-21, were induced with IPTG and lysed by sonication after addition of 10 ml TBST (20 mM Tris–Cl [pH 8.0], 200 mM NaCl, 0.25% Tween-20, 1 mM PMSF, 1 mM EDTA). Debris was removed by centrifugation, and the GST and GST fusion proteins were purified using glutathione beads (Pharmacia). Purified GST-N-TRP, GST-N-TRPL (0.1 μg each), or 0.2 μg GST (negative control) were immobilized on 20 μl glutathione–agarose beads (Pharmacia). [^{35}S]methionine-labeled N-TRP or N-TRPL probes were made by coupled transcription/translation using the TNT kit (Promega) and pN-TRP and pN-TRPL. Equal amounts of ^{35}S probe were incubated at 4°C for 1–2 hr with the glutathione beads, bound to either GST-N-TRP, GST-N-TRPL, or GST, in 200 μl TBST. The mixture was washed 3× in TBST with 350 mM NaCl, and the bound proteins were eluted with 20 mM glutathione. The elutes were fractionated by SDS–PAGE and transferred to PVDF membranes, and the ^{35}S-labeled proteins were detected using a phosphoimager (Fugix Inc.).

Isolation and Characterization of TRPC3

The EST clone R34716 (Wes et al., 1995) was used as a probe to screen a human-brain cDNA library (Clonetech) for full-length cDNAs. One positive clone, 3H, was isolated, which contained a 3.1 kb insert that included the full coding region.

Whole-Cell Recordings of Transfected 293T Cells

Subconfluent 293T cells were maintained in DMEM–FCS. The cells were recorded 36–48 hr after transfection. Before recording, CD4 beads were added as a marker to identify successfully transfected cells. Isolated cells with similar diameter and shape and therefore similar capacitivity (19.3–22.1 pF) were chosen for recording.

The whole-cell configuration was as described (Hamill et al., 1981). The pipette solution contained 140 mM CsCl, 2 mM $MgCl_2$, 10 mM EGTA, 0.3 mM ATP, 0.03 mM GTP, and 10 mM HEPES (pH 7.2). The pipette resistance was 2.5–3.0 MΩ. The cell-membrane potential was clamped at −60 mV for continuous observation. The cell capacity and series resistance were compensated before recording. After filtering at 3 kHz, the current was converted into digital data with a digiData 1200 interface (Axon Instruments). For studying the I–V relationship of the currents, a set of step voltage commands

(from −100 to +80 mV, in 15 mV increments) were applied to the cells clamped at −10 mV.

The cells were normally immersed in an extracellular solution (normal solution) containing 140 mM NaCl, 1.2 mM $MgCl_2$, 2.5 mM $CaCl_2$, 10 mM glucose, and 14 mM HEPES (pH 7.4), while other kinds of extracellular solutions were perfused through a 5-barrel drug-application system. To deplete the Ca^{2+} stores, the cells were perfused at least 7 min with 1 μM thapsigargin in normal solution containing 2.5 mM EGTA instead of $CaCl_2$. Three other extracellular solutions were also employed: the Na^+ solution contained 140 mM NaCl, 2.5 mM EGTA, 10 mM glucose, and 14 mM HEPES (pH 7.4); the Ca^{2+} solution contained 140 mM NMDG, 3 mM $CaCl_2$, 10 mM glucose, and 14 mM HEPES (pH 7.4); the NMDG solution, which was devoid of either Na^+, Ca^{2+}, or Mg^{2+}, contained 140 mM NMDG, 2.5 mM EGTA, 10 mM glucose, and 14 mM HEPES (pH 7.4). The osmolarity of all extracellular solutions was adjusted to 340 mosM with sucrose.

Leak currents were substracted only in those experiments in which we calculated the percent inhibition of the TRP- or TRPL-dependent currents by coexpression of the dominant-negative constructs. The leak currents used in these calculations were the mean current amplitudes of control cells at −100 mV, since the TRP- and TRPL-dependent currents in these experiments were also determined at −100 mV. The SDs were calculated according to the following equation in which X_i and X_{mean} represented the individual and mean values, respectively: $(\Sigma(X_i - X_{mean})/n)^{1/2}$.

For calculating the permeability ratios for P_{Ca}:P_{Na}, the current reversal potentials (V_{rev}) were measured when perfusing the cells with Na^+ solution (V_{rev-Na}) or Ca^{2+} solution (V_{rev-Ca}). After correcting the reversal potentials for junction potentials (Neher, 1992), the ratios were calculated according to the equation

$$P_{Ca}:P_{Na} = \frac{[Na^+]_o}{4[Ca^{2+}]_o} \times e^{F(2V_{rev\text{-}Ca} - V_{rev\text{-}Na})/RT}$$

which was derived from the following two equations:

$$V_{rev\text{-}Ca} = \frac{RT}{2F} \ln \frac{4P_{Ca}[Ca^{2+}]_o}{P_{cat}[cat]_i} \text{ and } V_{rev\text{-}Na} = \frac{RT}{F} \ln \frac{P_{Na}[Na^+]_o}{P_{cat}[cat]_i}$$

The P_{cat} and $[cat]_i$ represent the permeability and concentration of the intracellular monovalent cations, respectively.

Acknowledgments

We thank A. Choudhury and J. Yu for technical assistance, Drs. Z. Selinger for the TRPL antibodies, L. Feig for the 293T cells, M. Li for the *Shaker B* cDNA, CD4 plasmid, and anti-SHAKER B antibodies, and D. Gill , M. Li, K.-W. Yau, A. Kreuz, and P. Wes for critically reading the manuscript. This work was supported by a grant from the National Eye Institute (EY10852) to C. M.

Received April 10, 1997; revised May 22, 1997.

References

Arnon, A., Cook, B., Montell, C., Selinger, Z., and Minke, B. (1997). Calmodulin regulation of calcium stores in phototransduction of *Drosophila*. Science *275*, 1119–1121.

Berridge, M.J. (1995). Capacitative calcium entry. Biochem. J. *312*, 1–11.

Chevesich, J., Kreuz, A.J., and Montell, C. (1997). Requirement for the PDZ domain protein, INAD, for localization of the TRP store-operated channel to a signaling complex. Neuron *18*, 95–105.

Cosens, D.J., and Manning, A. (1969). Abnormal electroretinogram form a *Drosophila* mutant. Nature *224*, 285–287.

DuBridge, R.B., Tang, P., Hsia, H.C., Leong, P.M., Miller, J.H., and Calos, M.P. (1987). Analysis of mutation in human cells by using an Epstein-Barr virus shuttle system. Mol. Cell. Biol. *7*, 379–387.

Fields, S., and Song, O. (1989). A novel genetic system to detect protein–protein interactions. Nature *340*, 245–246.

Gillo, B., Chorna, I., Cohen, H., Cook, B., Manistersky, I., Chorev, M., Arnon, A., Pollock, J.A., Selinger, Z., and Minke, B. (1996). Coexpression of *Drosophila* TRP and TRP-like proteins in Xenopus oocytes reconstitutes capacitative Ca^{2+} entry. Proc. Natl. Acad. Sci. USA *93*, 14146–14151.

Hamill, O.P., Marty, A., Neher, E., Sakmann, B., and Sigworth, F.J. (1981). Improved patch-clamp techniques for high resolution current recording from cells and cell-free membrane patches. Pflügers Arch. *391*, 85–100.

Hardie, R.C. (1991). Whole-cell recordings of the light induced current in dissociated Drosophila photoreceptors, evidence for feedback by calcium permeating the light-sensitive channels. Proc. R. Soc. Lond. (B) *245*, 203–210.

Hardie, R.C., and Minke, B. (1992). The *trp* gene is essential for a light-activated Ca^{2+} channel in Drosophila photoreceptors. Neuron *8*, 643–651.

Hardie, R.C., and Minke, B. (1994). Calcium-dependent inactivation of light-sensitive channels in Drosophila photoreceptors. J. Gen. Physiol. *103*, 409–427.

Hardie, R.C., and Mojet, M.H. (1995). Magnesium-dependent block of the light-activated and *trp*-dependent conductance in Drosophila photoreceptors. J. Neurophysiol. *74*, 2590–2599.

Hartmann, H.A., Kirsch, G.E., Drewe, J.A., Taglialatella, M., Joho, R.H., and Brown, A.M. (1991). Exchange of conduction pathways between two related K^+ channels. Science *251*, 942–944.

Hoth, M., and Penner, R. (1992). Depletion of intracellular calcium stores activates a calcium current in mast cells. Nature *355*, 353–356.

Hu, Y., Vaca, L., Zhu, X., Birnbaumer, L., Kunze, D.L., and Schilling, W.P. (1994). Appearance of a novel Ca^{2+} influx pathway in Sf9 insect cells following expression of the transient potential-like (*trpl*) protein of Drosophila. Biochem. Biophys. Res. Commun. *201*, 1050–1056.

Huber, A., Sander, P., and Paulsen, R. (1996a). Phosphorylation of the *InaD* gene product, a photoreceptor membrane protein required for recovery of visual excitation. J. Biol. Chem. *271*, 11710–11717.

Huber, A., Sander, P., Gobert, A., Bähner, M., Hermann, R., and Paulsen, R. (1996b). The transient receptor potential protein (Trp), a putative store-operated Ca^{2+} channel essential for phosphoinositide-mediated photoreception, forms a signaling complex with NorpA, InaC and InaD. EMBO J. *15*, 7036–7045.

Jackson, T.R., Patterson, S.I., Thastrup, O., and Hanley, M.R. (1988). A novel tumour promoter, thapsigargin, transiently increases cytoplasmic free Ca^{2+} without generation of inositol phosphates in NG115–401L neuronal cells. Biochem. J. *253*, 81–86.

Jan, L.Y., and Jan, Y.N. (1992). Tracing the roots of ion channels. Cell *69*, 715–718.

Kozak, M. (1984). Compilation and analysis of sequences upstream from the translation start site in eukaryotic mRNAs. Nucleic Acids Res. *12*, 857–872.

Krause, E., Pfeiffer, F., Schmid, A., and Schulz, I. (1996). Depletion of intracellular calcium stores activates a calcium conducting nonselective cation current in mouse pancreatic acinar cells. J. Biol. Chem. *271*, 32523–32528.

Lewis, R.S., and Cahalan, M.D. (1989). Mitogen-induced oscillations of cytosolic Ca^{2+} and transmembrane Ca^{2+} current in human leukemic T cells. Cell Reg. *1*, 99–112.

Lückhoff, A., and Clapham, D.E. (1994). Calcium channels activated by depletion of internal calcium stores in A431 cells. Biophys. J. *67*, 177–182.

McDonald, T.V., Premack, B.A., and Gardner, P. (1993). Flash photolysis of caged inositol 1,4,5-trisphosphate activates plasma membrane calcium current in human T cells. J. Biol. Chem. *268*, 3889–3896.

Minke, B., and Selinger, Z. (1996). Role of Drosophila TRP in inositide-mediated Ca^{2+} entry. Mol. Neurobiol. *12*, 163–180.

Montell, C., and Rubin, G.M. (1989). Molecular characterization of the Drosophila *trp* locus: a putative integral membrane protein required for phototransduction. Neuron *2*, 1313–1323.

Montell, C., Jones, K., Hafen, E., and Rubin, G. (1985). Rescue of the *Drosophila* phototransduction mutation *trp* by germline transformation. Science *230*, 1040–1043.

Nakatani, K., and Yau, K.W. (1988). Calcium and magnesium fluxes across the plasma membrane of the toad rod outer segment. J. Physiol. *395*, 695–729.

Neher, E. (1992). Correction for liquid junction potentials in patch clamp experiments. In Ion Channels, B. Rudy and L.E. Iverson, eds. (San Diego, California: Academic Press, Inc.), pp. 123–131.

Niemeyer, B.A., Suzuki, E., Scott, K., Jalink, K., and Zuker, C.S. (1996). The Drosophila light-activated conductance is composed of the two channels TRP and TRPL. Cell *85*, 651–659.

Peterson, C.C.H., Berridge, M.J., Borgese, M.F., and Bennett, D.L. (1995). Putative capacitative calcium entry channels: expression of *Drosophila trp* and evidence for the existence of vertebrate homologues. Biochem. J. *311*, 41–44.

Philipp, S., Cacalié, A., Freichel, M., Wissenbach, U., Zimmer, S., Trost, C., Marquart, A., Murakami, M., and Flockerzi, V. (1996). A mammalian capacitative calcium entry channel homologous to Drosophila TRP and TRPL. EMBO J. *15*, 6166–6171.

Phillips, A.M., Bull, A., and Kelly, L.E. (1992). Identification of a Drosophila gene encoding a calmodulin-binding protein with homology to the *trp* phototransduction gene. Neuron *8*, 631–642.

Putney, J.W., Jr. (1986). A model for receptor-regulated calcium entry. Cell Calcium *7*, 1–12.

Putney, J.W., Jr., and Bird, G.St.J. (1993). The signal for capacitative calcium entry. Cell *75*, 199–201.

Salkoff, L., Baker, K., Butler, A., Covarrubias, M., Pak, M.D., and Wei, A. (1992). An essential "set" of K^+ channels conserved in flies, mice and humans. Trends Neurosci. *15*, 161–166.

Schwartz, T.L., Tempel, B.L., Papazian, D.M., Jan, Y.N., and Jan, L.Y. (1988). Multiple potassium-channel components are produced by alternative splicing at the Shaker locus in Drosophila. Nature *331*, 137–142.

Shieh, B.-H., and Zhu, M.-Y. (1996). Regulation of the TRP Ca^{2+} channel by INAD in Drosophila photoreceptors. Neuron *16*, 991–998.

Sinkins, W.G., and Schilling, W.P. (1997). Functional expression of TRPC1: A human homolog of the Drosophila TRP protein. Biophysical J. *72*, A271.

Suss-Toby, E., Selinger, Z., and Minke, B. (1991). Lanthanum reduces the excitation efficiency in fly photoreceptors. J. Gen. Physiol. *98*, 848–868.

Tinker, A., Jan, Y.N., and Jan, L.Y. (1996). Regions responsible for the assembly of inwardly rectifying potassium channels. Cell *87*, 857–868.

Vaca, L., Sinkins, W.G., Hu, Y., Kunze, D.L., and Schilling, W.P. (1994). Activation of recombinant *trp* by thapsigargin in Sf9 insect cells. Am. J. Physiol. *266*, C1501–C1505.

Wes, P.D., Chevesich, J., Jeromin, A., Rosenberg, C., Stetten, G., and Montell, C. (1995). TRPC1, a human homolog of a Drosophila store-operated channel. Proc. Natl. Acad. Sci. USA *92*, 9652–9656.

Wong, F., Schaefer, E.L., Roop, B.C., LaMendola, J.N., Johnson-Seaton, D., and Shao, D. (1989). Proper function of the Drosophila *trp* gene product during pupal development is important for normal visual transduction in the adult eye. Neuron *3*, 81–94.

Yellen, G., Jurman, M.E., Abramson, T., and MacKinnon, R. (1991). Mutations affecting internal TEA blockage identify the probable pore-forming region of a K^+ channel. Science *251*, 939–942.

Yool, A.J., and Schwarz, T.L. (1991). Alteration of ionic selectivity of a K^+ channel by mutation of the H5 region. Nature *349*, 700–704.

Zhu, X., Chu, P.B., Peyton, M., and Birnbaumer, L. (1995). Molecular cloning of a widely expressed human homologue for the *Drosophila trp* gene. FEBS Lett. *373*, 193–198.

Zhu, X., Jiang, M., Peyton, M., Boulay, G., Hurst, R., Stefani, E., and Birnbaumer, L. (1996). *trp*, a novel mammalian gene family essential for agonist-activated capacitative Ca^{2+} entry. Cell *85*, 661–671.

Zitt, C., Zobel, A., Obukhov, A.G., Harteneck, C., Kalkbrenner, F., Lückhoff, A., and Schultz, G. (1996). Cloning and functional expression of a human Ca^{2+}-permeable channel activated by calcium store depletion. Neuron *16*, 1189–1196.

Zweifach, A., and Lewis, R.S. (1995). Rapid inactivation of depletion-activated calcium current (I_{CRAC}) due to local calcium feedback. J. Gen. Physiol. *105*, 209–226.

GenBank Accession Number

The Genbank accession number for the *TRPC3* cDNA nucleotide sequence reported here is Y13758.